IJIE

The International Journal of Integrated Engineering

Study of Power Parameters of Forming Profile Elliptical Screw Workpieces

Oleg Lyashuk[1*], Andrii Diachun[2], Ivan Kuchvara[1], Yuriy Vovk[1], Volodymyr Dzyura[1]

[1]Department of Automobile Transport,
 Ternopil Ivan Puluj National Technical University 56 Ruska Str, Ternopil, 46001, UKRAINE

[2]Department of Mechanical Engineering, Ternopil Ivan Puluj National Technical University 56 Ruska Str, Ternopil, 46001, UKRAINE

*Corresponding Author

Abstract: Based on the power-saving technologies, the design of an installation for coiling elliptical screw workpieces is worked out. Theoretical dependences for determining power and structural parameters of coiling a screw profile workpiece (SPW) on the elliptical mandrel are developed with consideration of the material grade specification and the parameters of technological equipment. The dependences of the moment value of SPW bending to the elliptical mandrel on its rotation angle, thickness and width are defined. The challenge is to develop the progressive methods of manufacturing augers and their sub-type - L-shaped auger spirals (LSAS) with high precision geometrical dimensions Computer simulation of the tape workpiece winding process on ellipse mandrel with initial conditions, displacements, deformations and stresses that arising in the material of tape workpice after applying the simulated efforts to it, was shown. Given simulation showed ranges where maximum stresses of tension and compression arising in material of tape workpiece, and made it possible to determine the minimum radius of curvature during winding, which is advisable to take at least 20 mm.

Keywords: Elliptical screw, workpiece formation, coiling process

1. Introduction

The expansion of the range of various classes machine parts, in particular the screw ones, is characteristic for modern mechanical engineering. The working bodies' parts of screw conveyors and screw mixers are manufactured with the use of screw profile workpieces. These machines are widely used in construction, food and pharmaceutical processing industries, and particularly in agriculture to transport and mix bulk, viscous and other materials.

However, they possess additional qualities that, depending on the inclination of the spiral, can manifest themselves as the functions of increasing the resistance of transporting the materials to the surface of displacement, or vice versa - reducing the friction of transported material to the surface of displacement. In the first case, this phenomenon can be widely used in wiping or shredding different materials, and in the second - in separating and pruning various materials from the surface displacement.

The issue of manufacturing screw profile workpieces was studied in the works of Averkiev [1], Hevko [2], Kartika, Pontalier, and Rigal [3], Lyashuk et al [4], Lysov [5], Moshnin [6], Popov [7], Rene I.P. [8], Zubtsov [9] and many others.

The results of theoretical research of power parameters while forming the deflected outer contour of a crew workpiece are analysed in article [10]. The advances of L-shaped auger cleaners are substantiated.

Grigoriev A.M. and Preobrejenskiy P.A. [11], Hevko B.M. [2], Loveikin V. [12], and others investigated the procces of creating and operating the screw mechanisms; their works are dedicated to the issue of efficiency of auger conveyors. Pylypets M.I. [13], Hevko R.B. [14], and others researched the process of separating the root chaff [15-17]. Hevko I. [18] and other scientists researched the process of profiling screw spirals as well as the process of transportation by means of L-shaped augers.

However, existing screw working bodies cannot fully meet the performance requirements due to their high material consumption, high-energy costs and other disadvantages. The objective of this work is to develop the technological backgrounds of power-saving technologies for manufacturing highly efficient screw profile workpieces.

2. Research Methodology

Let us consider the process of coiling a profile L-shaped tape on the elliptical mandrel. The analytical model of this process is shown in Figure 1.
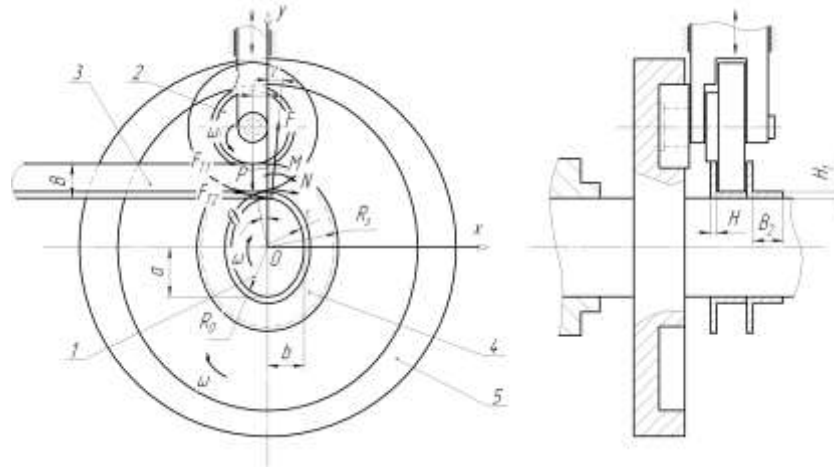

Fig. 1 - Analytical model of coiling a profile L-shaped tape on a mandrel: 1 – elliptical mandrel; 2 – clamp roller; 3 – profile L-shaped tape; 4 – profile elliptical screw element; 5 – socket cam of the same form with the elliptical mandrel 1 equidistance

During coiling, the profile tape fibers are compressed on the inner diameter of the edge of a screw profile elliptical element. The tape fibers on the outer diameter of this element are stretched. Having analysed the edges deformation in hot and cold states, the bending moment of the tape in these areas could be defined.

The radial stresses that occur in a zone of stretching the edge of a profile tape are defined by the Eq. 1 [2], [8], [13]:

$$\sigma_{\rho 1} = -\beta \sigma_S \cdot \ln \frac{R}{\rho}, \tag{1}$$

where β – coefficient that takes into account the impact of the average main stress equals 1.15;
σ_s – limit of material fluidity of the elliptical profile screw element MPa;
R – outer radius of bending, mm;
ρ – polar coordinate of bending radius, mm.

Similarly, the radial stresses in a compression zone are determined [6], [8]:

$$\sigma_{\rho 2} = -\beta \sigma_S \cdot \ln \frac{\rho}{r}, \tag{2}$$

where r – inner radius of bending, mm.

Tangential stresses in a zone of stretching:

$$\sigma_{\theta 1} = \beta \sigma_S \cdot \left(1 - \ln \frac{R}{\rho} \right). \tag{3}$$

142

Tangential stresses in a compression zone:

$$\sigma_{\theta 2} = -\beta \sigma_S \cdot \left(1 + \ln \frac{\rho}{r}\right). \tag{4}$$

The peculiarity of coiling the profile elliptical screw elements is the tape curvature radii and the tape bending radii, as they are variable during one rotation of the elliptical mandrel. Therefore, based on the equation of curvature radius of an ellipse [2], the inner bending radius of a workpiece r can be determined by the Eq. 5:

$$r = a^2 b^2 \left(\frac{y_0^2}{a^4} + \frac{x_0^2}{b^4}\right)^{\frac{3}{2}}, \tag{5}$$

where a – half of a major axis of the ellipse, *mm*;
b – half of a minor axis of the ellipse, *mm*;
x_0, y_0 – coordinates of the point, in which the curvature radius in coordinates system *XOY* is defined, mm.

The parametric equation of the ellipse is:

$$x = b \sin \theta$$
$$y = a \cos \theta \tag{6}$$

where θ – angle parameter within $0 \le \theta \le 2\pi$ that determines the rotation angle of the elliptical mandrel, rad.
Substituting the Eq. (6) into the Eq. (5), the following Eq. is deduced:

$$r = a^2 b^2 \left(\frac{\cos^2 \theta}{a^2} + \frac{\sin^2 \theta}{b^2}\right)^{\frac{3}{2}}. \tag{7}$$

Therefore, the outer radius R of bending the tape can be defined by the Eq.:

$$R = a^2 b^2 \left(\frac{\cos^2 \theta}{a^2} + \frac{\sin^2 \theta}{b^2}\right)^{\frac{3}{2}} + \beta_y B, \tag{8}$$

where β_y – shrinkage coefficient of a profile tape during coiling;
B – width of a profile tape edge, *mm*.

Bending moment of a profile tape edge can be determined by the formula:

$$M_1 = \left(\int\limits_{\rho_H}^{R} \sigma_{\theta 1} \rho d\rho + \int\limits_{r}^{\rho_H} \sigma_{\theta 2} \rho d\rho\right) H, \tag{9}$$

where ρ_H – radius of a neutral surface of tension, *mm*;
H – thickness of a profile tape edge, *mm*;

The radius of the neutral surface of tension is determined by the Eq. 10 [1]:

$$\rho_H = \sqrt{R\, r}. \tag{10}$$

Substituting Eq. (7), (8) into the Eq. (10), we obtain:

$$\rho_H = ab\left(\frac{\cos^2\theta}{a^2}+\frac{\sin^2\theta}{b^2}\right)^{\frac{3}{4}}\cdot\sqrt{a^2b^2\left(\frac{\cos^2\theta}{a^2}+\frac{\sin^2\theta}{b^2}\right)^{\frac{3}{2}}+\beta_y B}\ .\tag{11}$$

Substituting formulae (3), (4) into the formula (9) and considering the formula (10), we obtain:

$$M_1 = \beta\sigma_S\frac{H\beta_y^2 B^2}{4}\ .\tag{12}$$

Similarly, the bending moment of a profile tape shelf can be determined:

$$M_2 = \beta\sigma_S\frac{B_2 H_1^2}{4}\ ,\tag{13}$$

where H_1 – thickness of a profile workpiece shelf, mm;
B_2 – length of a profile workpiece shelf, mm.
  Then, the total bending moment of a profile L-shaped tape in hot condition:

$$M = \frac{\beta\sigma_S}{4}\left(H\beta_y^2 B^2 + B_2 H_1^2\right).\tag{14}$$

When the profile tape is being coiled on the elliptical mandrel in cold condition, the tape material is being strengthened. Besides, the value of tangential stresses for the profile tape edge is determined by formulae [8]:
  • in a zone of stretching:

$$\sigma_{\theta 1} = \beta\left[\sigma_{TO}\left(1-\ln\frac{R}{\rho}\right)+\frac{\Pi}{2}\left(2\ln\frac{\rho}{\rho_H}-\ln\frac{\rho R}{\rho_H^2}\ln\frac{R}{\rho}\right)\right];\tag{15}$$

  • in a zone of compression:

$$\sigma_{\theta 2} = -\beta\left[\sigma_{TO}\left(1+\ln\frac{\rho}{r}\right)+\frac{\Pi}{2}\left(2\ln\frac{\rho_H}{\rho}+\ln\frac{\rho_H^2}{\rho r}\ln\frac{\rho}{r}\right)\right],\tag{16}$$

where σ_{T0} – extrapolated limit of tape material fluidity, MPa;

Π – linear module of strengthening the tape material, MPa.
  Substituting the Eq. (7), (8), (15), (16) into the equation (9), the bending moment of a profile tape edge is defined after integration and reductions:

$$M_1 = \beta H \left[\sigma_{TO} \frac{\beta_y^2 B^2}{4} + \Pi \left(\frac{2a^4b^4 \left(\frac{\cos^2 \theta}{a^2} + \frac{\sin^2 \theta}{b^2} \right)^3 + 2a^2b^2 \left(\frac{\cos^2 \theta}{a^2} + \frac{\sin^2 \theta}{b^2} \right)^{\frac{3}{2}} \beta_y B + \beta_y^2 B^2}{4} \times \right. \right.$$

$$\left. \left. \times \ln \sqrt{1 + \frac{\beta_y B}{a^2 b^2 \left(\frac{\cos^2 \theta}{a^2} + \frac{\sin^2 \theta}{b^2} \right)^{\frac{3}{2}}}} - \frac{2a^2b^2 \left(\frac{\cos^2 \theta}{a^2} + \frac{\sin^2 \theta}{b^2} \right)^{\frac{3}{2}} \beta_y B + \beta_y^2 B^2}{8} \right) \right]. \tag{17}$$

Considering the Eq. (7), a simplified Eq. (17) is deduced:

$$M_1 = \beta H \left[\sigma_{TO} \frac{\beta_y^2 B^2}{4} + \Pi \left(\frac{2r^2 + 2r\beta_y B + \beta_y^2 B^2}{4} \cdot \ln \sqrt{1 + \frac{\beta_y B}{r}} - \frac{2r\beta_y B + \beta_y^2 B^2}{8} \right) \right]. \tag{18}$$

While coiling, the profile tape shelf forms a cylindrical surface. The connections from the side of a deformed edge are overlapped on the ends of this surface. Thus, the plane-strain state [8] is implemented for the profile tape shelf. Besides, the shelf is completely in a compression zone, so, the equation for determining the bending moment of a profile tape shelf can be deduced:

$$M_2 = B_2 \int_r^{r_2} \sigma_{\theta 2} \rho d\rho. \tag{19}$$

where r_2 – outer radius of bending the shelf, mm; $r_2 = r + H_1$.

Substituting the equation (16) into the equation (19), the bending moment of a profile tape shelf can be deduced:

$$M_2 = \frac{1}{2} \beta B_2 \left[\sigma_{TO} \left(r_2^2 \left(\ln \frac{r_1}{r_2} - \frac{1}{2} \right) + \frac{1}{2} r_1^2 \right) + \Pi \left(r_1^2 \left(\ln \frac{\sqrt{r_1} \sqrt{\rho_i}}{2} - \frac{1}{4} \right) + \right. \right.$$

$$\left. \left. + r_2^2 \left(\frac{1}{2} (\ln r_2)^2 + \frac{1}{4} + \ln \frac{2}{\sqrt{r_2} \sqrt{\rho_i}} + \ln \rho_i \ln \frac{r_1}{r_2} - \frac{1}{2} (\ln r_1)^2 \right) \right) \right] \tag{20}$$

Then, the total bending moment of bending the profile L-shaped tape in cold condition:

$$M = \beta H \left[\sigma_{TO} \frac{\beta_y^2 B^2}{4} + \Pi \left(\frac{2r^2 + 2r\beta_y B + \beta_y^2 B^2}{4} \cdot \ln \sqrt{1 + \frac{\beta_y B}{r}} - \frac{2r\beta_y B + \beta_y^2 B^2}{8} \right) \right] +$$

$$+ \frac{1}{2} \beta B_2 \left[\sigma_{TO} \left(r_2^2 \left(\ln \frac{r_1}{r_2} - \frac{1}{2} \right) + \frac{1}{2} r_1^2 \right) + \Pi \left(r_1^2 \left(\ln \frac{\sqrt{r_1} \sqrt{\rho_i}}{2} - \frac{1}{4} \right) + \right. \right.$$

$$\left. \left. + r_2^2 \left(\frac{1}{2} (\ln r_2)^2 + \frac{1}{4} + \ln \frac{2}{\sqrt{r_2} \sqrt{\rho_i}} + \ln \rho_i \ln \frac{r_1}{r_2} - \frac{1}{2} (\ln r_1)^2 \right) \right) \right]. \tag{21}$$

Based on Eq. (7), (11), (21), the following conclusions should be made. First, when the profile tape is being coiled on the elliptical mandrel in cold condition, the moment of bending the tape from the rotation angle of elliptical mandrel is being changed. Second, the greatest bending moment occurs when the rotation angle is $\theta = 0, \pi$ radians; the smallest bending moment occurs when the rotation angles are $\theta = \frac{1}{2}\pi, \frac{3}{4}\pi$ radians.

According to the analytical model shown in Fig. 1, the equilibrium equation of the profile tape part, which undergoes the deformation, can be written as follows [9]:

$$\left. \begin{array}{l} \text{along the axis} \quad \text{x} : -F_{T1} - F_{T2} \cdot \cos \gamma + N \cdot \cos \gamma + F \sin \gamma = 0 \\ \text{along the axis} \quad \text{y} : -P + F_{T2} \cdot \sin \gamma - N \cdot \sin \gamma + F \cos \gamma = 0 \\ \text{sum moment} : P \cdot l + F_{T1} \cdot R_3 + F_{T2} \cdot R_0 - N \cdot \rho_H - M = 0 \end{array} \right\} \tag{22}$$

where F_{T1} – friction force between the roller and profile tape, N;

F_{T2} – friction force between the profile tape and elliptical mandrel, N;

γ – pressure angle of the elliptical mandrel, *grad*;

N – longitudinal force, N;

F – resultant of normal contact stresses on the profile tape, N;

P – force of bending by a clamping roller, N;

l – distance between the centres of the elliptical mandrel and clamping roller, *mm*;

R_3 – outer radius of interaction of the elliptic screw element relative to the centre of rotation of the elliptical mandrel, *mm*;

R_0 – distance from the centre of mandrel rotation to its surface, *mm*.

The friction forces are determined by the dependencies:

$$F_{T1} = \mu_1 \cdot P ; \tag{23}$$

$$F_{T2} = \mu_2 \cdot F , \tag{24}$$

where μ_1 – coefficient of friction between the clamping roller and the tape;

μ_2 – coefficient of friction between the elliptic mandrel and the elliptic screw element.

The resultant of normal contact stresses is defined by the formula:

$$F = \sigma_r \cdot H \cdot L , \tag{25}$$

where σ_r – contact normal stresses along the inner radius of the elliptic screw element, *MPa*;

L – contact length along the inner diameter of the elliptic screw element, *mm*.

Providing that the bending moment is known, the forces that occur during coiling can be determined by solving the system of Eq. (22). In this case

$$F = \frac{-P \cdot \left(\mu_1 \cdot tg\gamma - 1 \right)}{\mu_2 \cdot \sin \gamma + tg\gamma \cdot \left(-\mu_2 \cdot \cos \gamma + \sin \gamma \right) + \cos \gamma} ; \tag{26}$$

$$N = \frac{\mu_1 \cdot P + F \cdot \left(\mu_2 \cdot \cos \gamma + \sin \gamma \right)}{\cos \gamma} . \tag{27}$$

According to experimental studies, the maximum bending force P by a clamping roller occurs at the initial stage of deformation, that is, when the angle γ is zero. Therefore, to simplify the calculations, the system of Eq. (22) will be solved as follows:

$$P = F ; \tag{28}$$

$$N = (\mu_1 + \mu_2) \cdot P; \tag{29}$$

$$P = \frac{M}{l + \mu_1 R_3 + \mu_2 R_0}. \tag{30}$$

The distance from the centre of mandrel rotation to its surface is determined by the formula:

$$R_0 = \sqrt{a^2 \cos^2 \theta + b^2 \sin^2 \theta}. \tag{31}$$

The outer radius of interaction of the screw element relative to the centre of mandrel rotation is determined by the formula [9]:

$$R_3 = \sqrt{(a+B)^2 \cos^2 \theta + (b+B)^2 \sin^2 \theta}. \tag{32}$$

It should be noted that in this case the friction coefficient angle μ_1 between the clamping roller and profile tape is a specific value and does not meet the immediate value of the friction coefficient for contacting materials. The moment that must be applied to rotate the elliptic mandrel, depends on their structural features and is generally determined according to the dependence shown in Figure 1:

$$M_0 = k_M \cdot P \cdot (l + \mu_1 \cdot R_3) \tag{33}$$

where k_M – coefficient considering design performance of the mandrel.

Based on the above formula, the necessary technological equipment can be designed. Thus, to reduce the torque of elliptical mandrel, and hence to reduce the required power of coiling elliptical screw workpieces, the friction coefficient should be minimized, for example, using lubricants.

The derived dependencies should be calculated using the package of applications for PC. Based on calculations results, the dependency graphs of bending force and torque on the rotation angle of elliptical mandrel are drawn (Figure 2, 3).
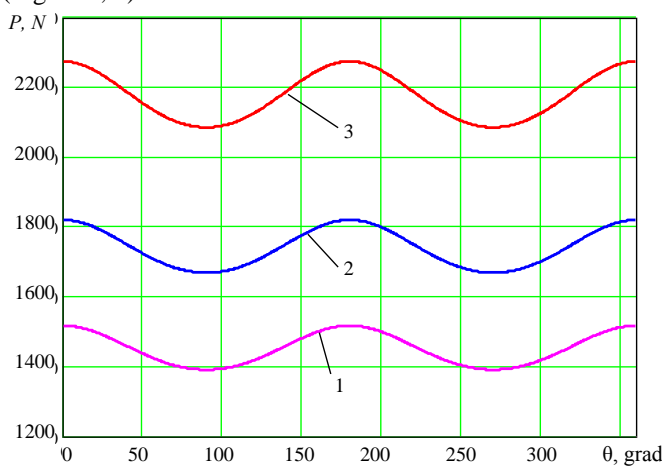

Fig. 2 - Dependency graphs of the bending force by clamping roller on the rotation angle of the elliptical mandrel (St3, σᵥ = 440 MPa) B = 15 mm; a = 50 mm; b = 40 mm; B₂=12 mm, H=H1: 1 – H=1 mm; 2 – H=1.2 mm; 3 – H=1.5 mm
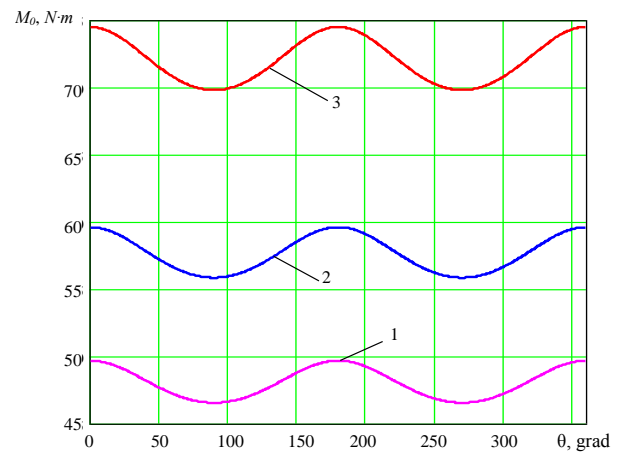
Fig. 3 - Dependency graphs of the moment that should be applied to rotate the elliptical mandrel on the mandrel rotation angle (St3, σᵥ=440 MPa) B = 15 mm; a=50 mm; b=40 mm; B₂=12mm, H=H₁: 1 – H=1 mm; 2 – H=1.2 mm; 3 – H=1.5 mm

The forces and the formation moment assume maximum value during the workpiece formation on the elliptical mandrel part from the major sub-axis side and therefore comes to the minor axis of the ellipse.

Based on the above calculations, the dependency graphs of the bending force and torque to form an elliptical screw element on the tape thickness H are developed (Figure 4 and Figure 5).
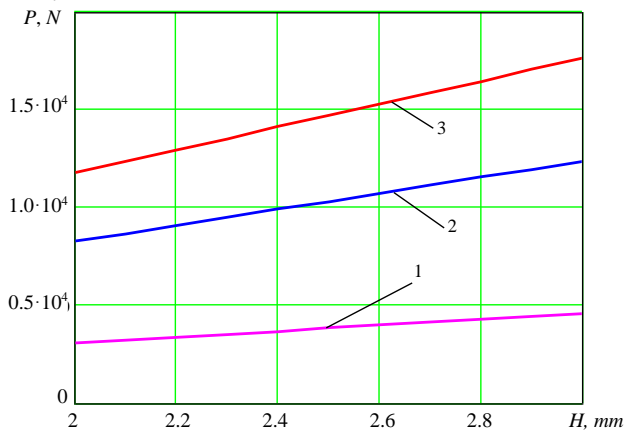
147

Fig. 4 - Dependency graphs of maximum bending force by a clamping roller on the tape thickness (St 3, σ_v = 440MPa) a = 50 mm; b = 40 mm, B_2= 12mm, H = H_1: 1 – B = 15mm; 2 – B = 25mm; 3 – B = 30mm

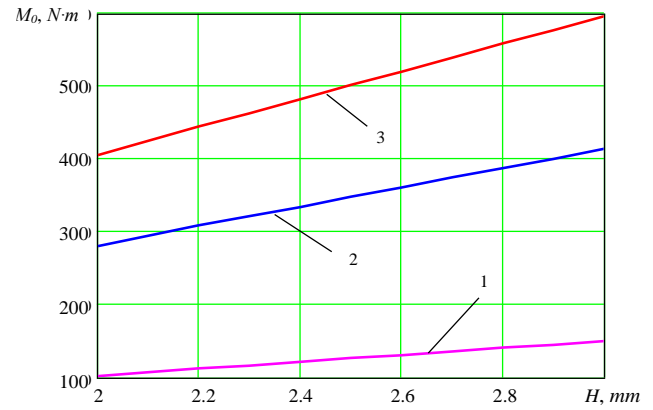**Fig. 5 - Dependency graphs of the moment, which must applied to rotate the elliptical mandrel on the tape thickness (St3, σ_v = 440MPa) a = 50 mm; b= 40 mm, B_2= 12mm, H = H_1: 1 – B = 15mm; 2 – B = 25mm; 3 – B = 30mm**

3. Results and Discussion

The experimental installation, general view of which is presented on Figure 6, was designed for experimental investigations conducting.
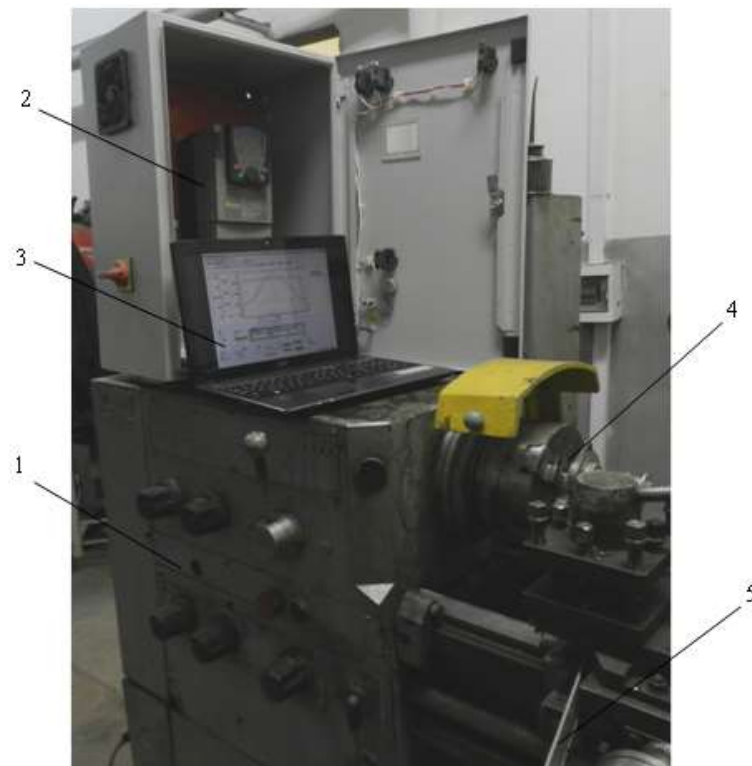

Fig. 6 - General view: 1 – turning machine; 2 – Altivar 71; 3 – PC; 4 – device for winding elliptical screw elements with a given step; 5 – tape workpiece

Torque value and engine power were recorded in percentages from rated. Engine power was determined by rated engine power (7.5 kW) and maximal percentage value for selected mode multiplication.

Regressive dependence, for determining the dependence of bending force on clamping roller from changing of three main factors: tape thickness H, tape width B and the half of lower axis of the ellipse b for materials St 3, and aluminum alloy D16 during elliptical screw elements shaping, based on multifactorial experiment was received.

- for tape material St3

$$P_{(H,B,b)} = 2496.2 - 1468.15H - 366.09B + 67.23b + 228.06HB - $$
$$-25.08Hb - 4.65Bb + 4.16H^2 + 11.68B^2 + 0.56b^2$$

(34)

- for tape material aluminum alloy D16

$$P_{(H,B,b)} = 3087.4 - 1773.9H - 431.27B + 73.72b + 269.34HB - $$
$$-29.25Hb - 5.54Bb + 8.64H^2 + 13.8B^2 + 0.75b^2$$

(35)

It was found that the main factor which affects on determining of bending force on clamping roller during elliptical screw elements shaping in such limits of input factors change: $2 \leq H \leq 3$ (*mm*); $16 \leq B \leq 30$ (*mm*); $32 \leq b \leq 42$ (*mm*) with half of ellipse larger axis *a*= 45 *mm*.

On the Figure 6 response surfaces of value *P* changing from simultaneous change of two factors: a – *P = f(H,B)*; b– *P = f(H,b)*; c – *P = f(B,b)* were shown.
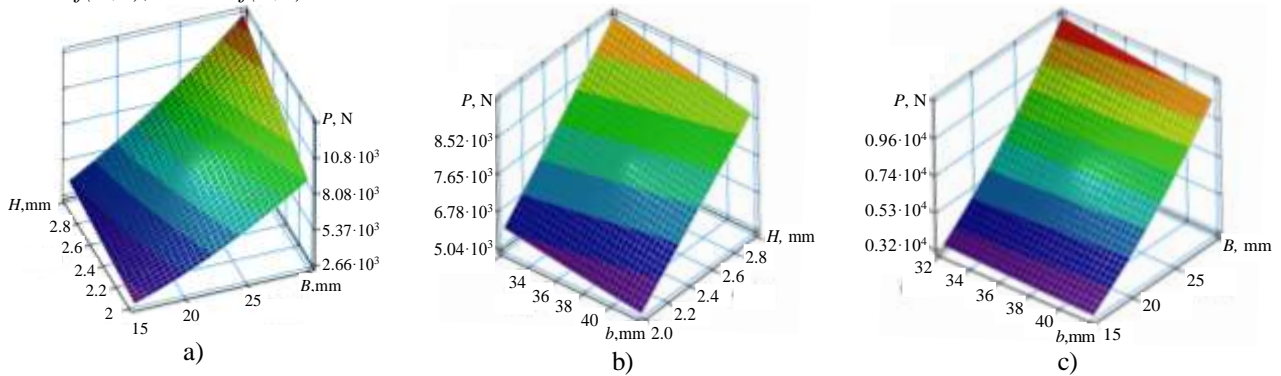

Fig. 7 - **Response surface of dependence bending force on clamping roller from variable factors during elliptical screw elements shaping, made with St3**

From graphical data (Figure 6) it is visible that for St3 with *H*=3 *mm*, *b*=37 *mm* and changing *B* on limits 20-30 *mm* bending force acquires values $0.41 \cdot 10^4$-$0.9 \cdot 10^4$ *N*; but for aluminum alloy D16 with changing *B* on limits 20-30 *mm* bending force increases in 2.27 times from $0.47 \cdot 10^4$ *N* to $1.065 \cdot 10^4$ *N*, with *H*=3 mm, *b*=37 *mm*.

Computer simulation to establish the relationship between force efforts and the corresponding deformations was conducted for choosing the rational design parameters of the tape minimum permissible bending radius.

A computer simulation of the tape permissible bending radius was applied and graphical representation of displacement, deformation and stresses that arising in material of the tape workpiece under the applied efforts were presented with the application package of SolidWorks.
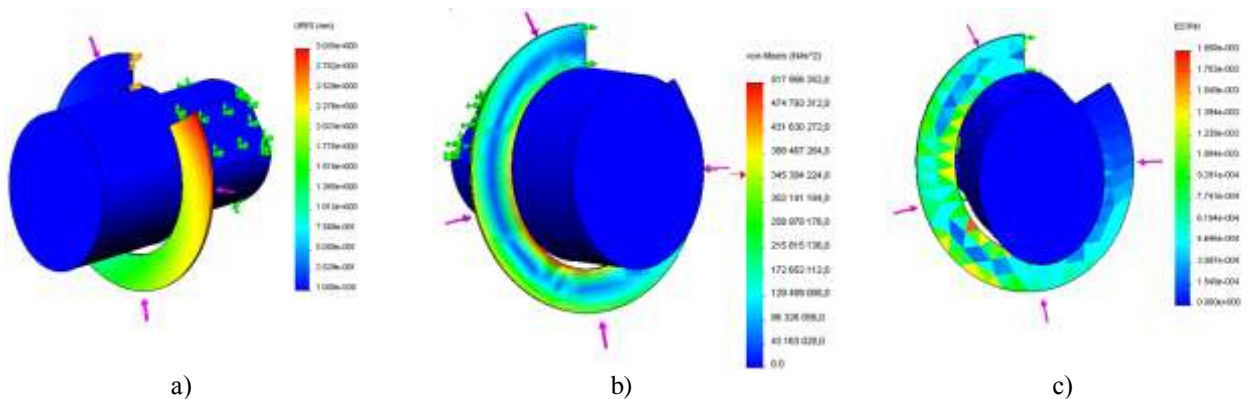

Fig. 8 - **(a) Graphic display of displacement; (b) tension; (c) deformation, that arising in the material of the tape workpiece under the applied efforts**

Based on presented computer simulation we can notice that the changes of stresses that arising in material of the tape workpiece dependence from curvature of the bending radius for St 3 $\sigma_v = 440$ *MPa* and aluminum alloy D16 $\sigma_v = 520$ *MPa*. From graphical data it is visible that with increasing bending radius of the tape, the stresses that arising in its material are decreasing, and when the value of the radius is equal *r* = 16 *mm* acquire unacceptably large values,

which leads to the destruction of the material. Therefore it is advisable to use elliptical mandrel with minimum curvature radius at least 20-25 *mm*.

4. Conclusions

Based on theoretical studies, the analytical dependences for determining the power parameters of coiling a SPW on the elliptical mandrel with consideration of the material grade specification and the parameters of technological equipment are developed.

The dependences of the bending moment value of the elliptical mandrel on the angle of rotation, the thickness and width are defined. The dependences of the moment value of SPW bending to the elliptical mandrel on its rotation angle, the thickness and width are developed.

According to graphic dependences in Figure 2 and Figure 3, the bending force of a profile tape by a clamping roller is within P=1390-1520 N and the bending moment is M_0=46-49.5 $N{\cdot}m$, provided that the tape thickness is H=1 *mm*. While coiling the tape with a thickness H=1.5 *mm* on the elliptical mandrel, the bending force is within P=2100-2250 N, and the moment M_0=70-74.5 $N{\cdot}m$.

Acknowledgement

References

[1] Averkiev, Y. A. (1984). The nature of the shape change and force conditions of bending the tape to the rib. Mechanical Engineering News, 1, 64-66

[2] Hevko, B. M. (1986). Technology of manufacturing screw augers. Lviv, USSR: Vyshcha shkola

[3] Kartika, A., Pontalier, P.Y. and Rigal, L. (2006). Extraction of sunflower oil by twin screw extruder: Screw configuration and operating condition effects. Bioresource Technology, 97(18), 2302-2310, https://doi.org/10.1016/j.biortech.2005.10.034

[4] Lyashuk, O., Sokil, M., Vovk, Y., Levkovych, M., Tson, O., Kondratyuk, D. and Dmytrenko, V. (2019). Analysis of resonance oscillations of extruder elastic screw conveyor. International Journal of Engineering Research in Africa, 43, 49-58

[5] Lysov, M. I. (1966). Theory and calculation of the processes of manufacturing parts by bending. Moscow, USSR: Mechanical Engineering

[6] Moshnin, Y. M. (1977). Bending and straightening by rotary machines. Moscow, USSR: Mechanical Engineering.

[7] Popov, Y. A. (1980). Fundamentals of the theory of sheet stamping. Moscow, USSR: Mechanical Engineering

[8] Renne, I. P. (1950). Plastic bending of a sheet billet. Proceedings of the Tula Mechanic Institute, 4, 142-162.

[9] Zubtsov, M. Y. (1980). Sheet stamping. Leningrad, USSR: Mechanical Engineering

[10] Hevko, I., Kuchvara, I., Diachun, A. and Hupka, A. (2015). Study of the force parameters of shaping the profile screw elements. MOTROL. Commission of Motorization and Energetics in Agriculture, 17(7), 111-116

[11] Grigoriev A.M. and Preobrejenskiy P.A. (1967). Complex mechanization and automation of cargo handling and transport operations in engineering and instrument. Naukova Dumka

[12] Loveikin, V., Chovniuk, Yu. and Kulyk, V. (2012). Optimizatsiia rezhimov kolebanii zernovykh smesei pri nalichii sukhogo treniia. Motrol – Motoryzacja i energetyka rolnictva, 14(3), 140-149

[13] Pylypets M. I. (2002). Scientifically and technological bases of production coiling machine parts billet: Author. Lviv: PhD Thesis Engineering Sciences specials, 35

[14] Hevko, R. B., Strishenets, O. M., Lyashuk, O. L., Tkachenko, I. G., Klendii, O.M. and Dzyura, V.O. (2018). Development of a pneumatic screw conveyor design and substantiation of its parameters. INMATEH: Agricultural engineering, 54(1), 153-160

[15] Lyashuk, O., Sokil, M., Vovk, Y., Gupka A. and Marunych O. (2018). Torsional oscillations of an auger multifunctional conveyor's screw working body with consideration of the dynamics of a processed medium continuous flow. Ukrainian Food Journal, 7(3), 499-510

[16] Lutsak, D, Prysyazhnyuk, P, Burda, M. and Aulin, V. (2016). Development of a method and an apparatus for tribotechnical tests of materials under loose abrasive friction. Eastern-European Journal of Enterprise Technologies, 5(7-83), 19-26

[17] Aulin, V., Arifa, W., Lysenko, S. and Kuzyk, A. (2016). Improving of the wear resistance of working parts agricultural machinery by the implementation of the effect of self-sharpening. International Journal of Engineering and Technology, 5(4), 126-130

[18] Hevko, I. B., Dyachun, A. Ye., Hud, V. Z., Rohatynska, L. R. and Klendiy, V. M., (2015). Investigation of the stability of the tonsorial vibration of a screw conveyer under the influence of pulse forces. INMATEH-Agricultural Engineering, 45(1), 77-86